Improved ductility of aged Mg-9Al-1Zn alloy strip by electropulsing treatment

Yanbin Jiang
Advanced Materials Institute, Graduate School at Shenzhen, Tsinghua University, Shenzhen 518055, People's Republic of China; and Department of Physics and Materials Science, City University of Hong Kong, Kowloon Tong, Hong Kong

Guoyi Tang[a)]
Advanced Materials Institute, Graduate School at Shenzhen, Tsinghua University, Shenzhen 518055, People's Republic of China

Chanhung Shek
Department of Physics and Materials Science, City University of Hong Kong, Kowloon Tong, Hong Kong

Yaohua Zhu
Department of Industrial and Systems Engineering, Hong Kong Polytechnic University, Kowloon, Hong Kong

Lei Guan, Shaonan Wang, and Zhuohui Xu
Advanced Materials Institute, Graduate School at Shenzhen, Tsinghua University, Shenzhen 518055, People's Republic of China

(Received 12 October 2008; accepted 23 January 2009)

The effect of electropulsing treatment (EPT) on the microstructure and mechanical properties of aged Mg-9Al-1Zn alloy strip was studied. EPT was found to accelerate tremendously the β phase spheroidization in the aged Mg-9Al-1Zn alloy. This improved microstructure exhibits excellent mechanical properties, that is, increasing elongation to failure significantly without loss of tensile strength. The spheroidization of the β phase during EPT was attributed to the reduction of the nucleation thermodynamic barrier and enhancement of atomic diffusion.

I. INTRODUCTION

In recent years, Mg-9Al-1Zn alloy (AZ91) has attracted a lot of attention due to its excellent properties, such as low density, high specific strength, and good damping capacity. However, the AZ91 alloy exhibits low strength and low ductility at room temperature compared to other commercial structural materials, such as Al alloys and steel. These considerably inhibit AZ91's widespread application. Some research focused on grain refinement of AZ91 using severe plastic deformation (SPD) techniques,[1–3] including equal channel angular pressing (ECAC)[4,5] and accumulative roll bonding (ARB),[6–8] which can improve both the strength and ductility. Nevertheless, SPD techniques have difficulty satisfying industrial needs due to their low production efficiency and high manufacturing cost. In the present work, a novel technique of electropulsing treatment (EPT)[9,10] is applied to an aged AZ91 strip for improving ductility without any compromise in tensile strength. EPT accelerated spheroidization of the strengthening β phase tremendously in the aged AZ91 alloy strip. Finally, the mechanism of the effect is discussed.

II. EXPERIMENTAL

A commercial magnesium alloy AZ91 (9.1wt%Al, 0.9wt%Zn, 0.2wt%Mn, balance Mg) was used. The ingot was homogenized at 673 K for 16 h, and subsequently extruded into strip of width 2.90 mm and thickness 1.45 mm. The extruded strip was then electropulsing-rolled[11] to 1.00 mm thick. The rolled strip was aged for 12 h at 493 K to obtain the as-aged strip consisting of α-Mg and β-$Mg_{17}Al_{12}$. The as-aged strips were subjected to EPT with various parameters of electropulsing, as listed in Table I. For comparison, the as-aged strips were heated up to 723 K over the course of about 8 s in a furnace, followed by natural cooling in air. The average heating rate was about 90 K/s, and this simulated the thermal effect during EPT. These samples were referred to as AT samples.

The EPT process is schematically shown in Fig. 1. The AZ91 strip was on-line treated by multiple electropulsing, when the strip was moving at a speed of 2 m/min

[a)]Address all correspondence to this author.
e-mail: tanggy@mail.tsinghua.edu.cn
DOI: 10.1557/JMR.2009.0197

TABLE I. Experimental EPT parameters for treatment of the aged AZ91 strip.

Sample number	Frequency (Hz)	Duration (μs)	j_m (A/mm^2)	j_e (A/mm^2)	Measured temperature near the cathode (K)
EPT1	92	80	326	18.6	403
EPT2	111	80	330	20.6	445
EPT3	121	80	339	22.0	463
EPT4	153	80	339	24.8	498
EPT5	200	80	331	27.9	528
EPT6	221	80	335	29.1	573

Note: j_m is the amplitude of current density of electropulsing; j_e represents the RMS value of current density during EPT and is related to the Joule heating effect.

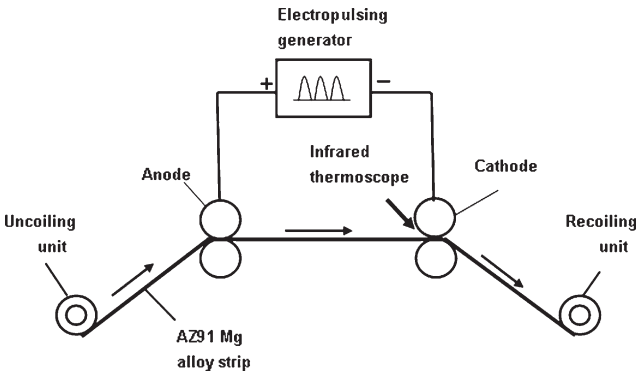

FIG. 1. Schematic view of the EPT process.

through a distance of 225 mm between the two electrodes. A self-made electropulsing generator was applied to discharge the positive direction multiple pulses. It took about 7 s to move the strip from the anode to the cathode. The pressure between the electrodes and the strip was just sufficient to keep good electrical contact without causing deformation of the strip. Electropulses with various frequencies and pulse durations (from 70 to 80 μs) were applied to the strip. The current parameters including frequency, root-mean-square current (RMS), amplitude, and duration of current pulses were monitored by a Hall Effect sensor connected to an oscilloscope. The temperature of the AZ91 strip near the cathode was measured using a Raytek MX2 infrared thermoscope. The EPT6 sample experienced an average heating rate of 83 K/s during EPT, which was comparable to that of the AT sample.

A JSM-820 JEOL scanning electron microscope (SEM) was used to observe the microstructure of the samples. The transverse sections of the strips were polished and etched for microstructure observation in SEM. The phases in the samples were identified by x-ray diffraction (XRD) using a Philips X'Pert Diffractometer with Cu K_α radiation. A uniaxial tensile test at room temperature was carried out at a rate of 2 mm/min, using the strip specimens with a gauge length of 50 mm. Five samples of each condition were tested.

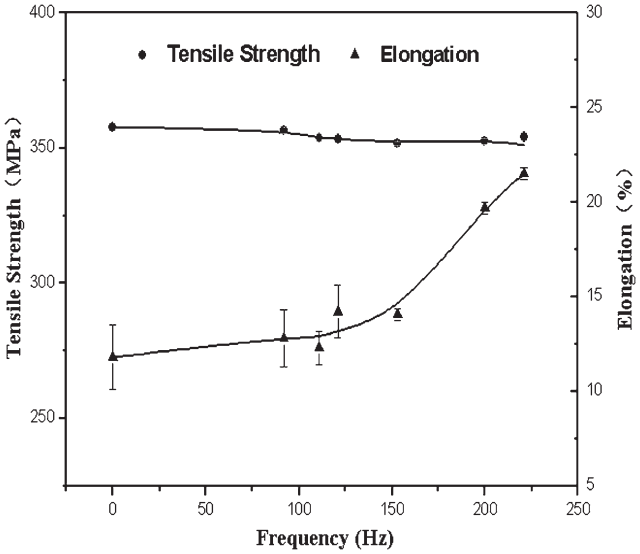

FIG. 2. The relationship between tensile strength, elongation, and frequency of electropulsing of samples.

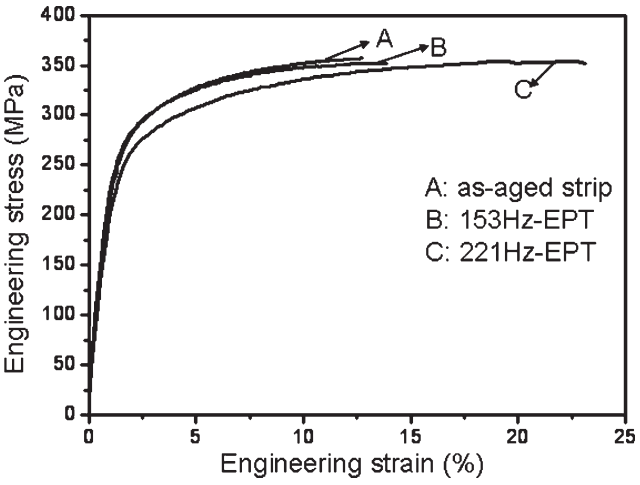

FIG. 3. Engineering stress-strain curves of the as-aged, 150 Hz-EPT and 221 Hz-EPT samples.

III. EXPERIMENTAL RESULTS

The relationship between temperature and frequency of electropulsing is shown in Table I. It was found that the temperature of EPT samples rose with increasing frequency of electropusling due to the Joule heating effect. Figures 2 and 3 show the relationship between tensile strength, elongation to failure, and frequency of electropulsing of samples. The tensile strength of the samples remained almost unchanged, while the yield strength decreased slightly, when the frequency of electropulsing increased. To the contrary, the elongation to failure of the samples increased remarkably with frequency of electropulsing. The elongation of the sample treated by 221 Hz-EPT approached 21.5%, which corresponded to an 82% increase compared with that of the as-aged sample (11.8%). EPT improved the

plasticity of the as-aged AZ91 strips effectively without compromising the tensile strength.

XRD patterns for the as-aged sample, the AT sample, and the EPT samples are shown in Fig. 4. The as-aged sample consisted of mainly two phases, namely, α-Mg and β-$Mg_{17}Al_{12}$. With increasing frequency of electropulsing, the peaks of the β phase weakened. This implies that the β phase transformed gradually with increasing frequency of electropulsing during EPT. However, XRD analysis also shows that the AT sample had very similar XRD patterns to the as-aged sample. This indicates that the amount of β-$Mg_{17}Al_{12}$ was not reduced in the AT sample by conventional heat treatment with a similar heating rate to EPT with a frequency of 221 Hz.

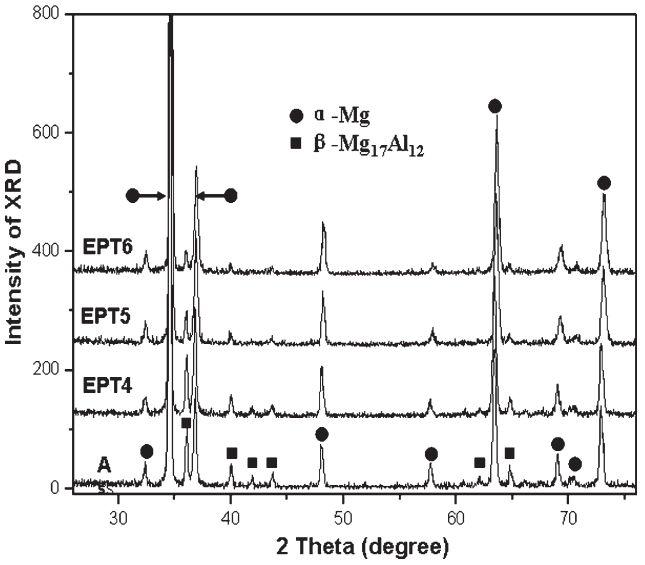

FIG. 4. XRD patterns for samples at various conditions.

The microstructure changes of the as-aged sample before and after the 221 Hz-EPT are shown in Fig. 5. The matrix was α-Mg and the precipitates were β-$Mg_{17}Al_{12}$. For the as-aged sample, numerous β particles precipitated at grain boundaries and inside the grains, and many β lamellar clusters were formed, as indicated by the arrows in Figs. 5(a) and 5(b). After 221 Hz-EPT, the β lamellar clusters disappeared and a large amount of spherical β particles formed uniformly in the sample, as shown in Fig. 5(c). This agrees well with the XRD results. Furthermore, the α-Mg matrix grains did not grow appreciably during EPT. This means that EPT tremendously accelerated the spheroidization of the β phases in the as-aged AZ91 strip during a very short period of 7 s. However, numerous β lamellar clusters remained in the AT sample (by conventional heat treatment), as shown in Fig. 5(d). The SEM results were in good agreement with the XRD analysis.

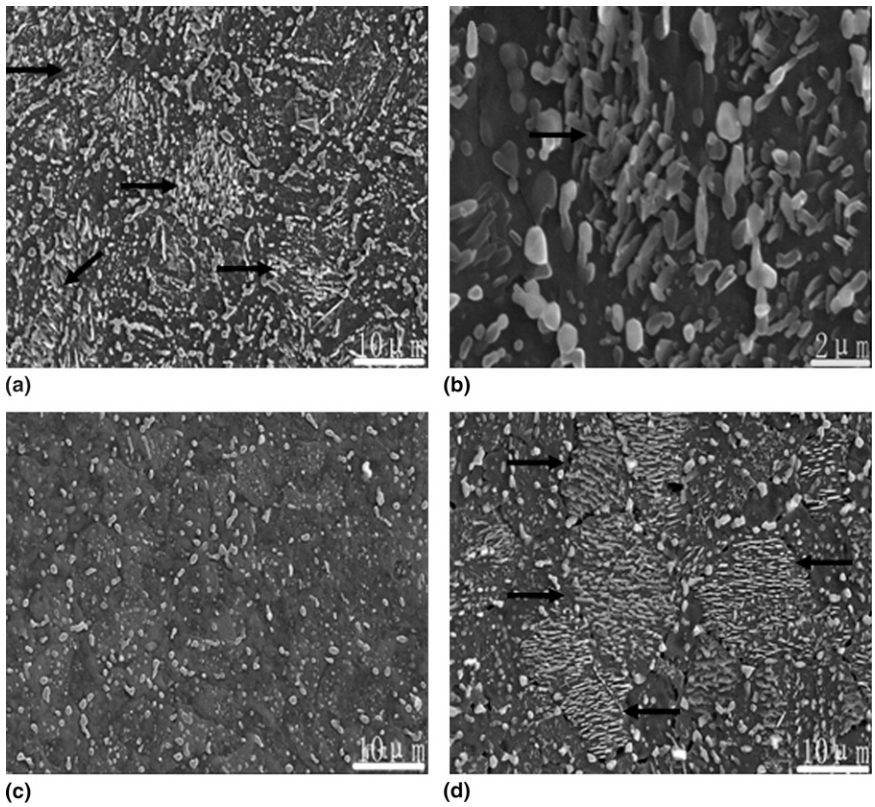

FIG. 5. SEM micrographs of samples: (a) as-aged sample (low magnification); (b) as-aged sample (high magnification); (c) sample EPT6 (221 Hz); (d) sample AT.

IV. DISCUSSION

The dense β lamellar clusters existing in the α-Mg matrix induced a large local stress concentration around the clusters and resulted in premature fracture of the samples when force is applied on the samples. Such behavior severely reduced both the plasticity and formability of the as-aged AZ91 strip. After 221 Hz-EPT, the β lamellar clusters disappeared and numerous spherical β particles were distributed uniformly in the α-Mg matrix. Such microstructure favorably released the internal stress and reduced the probability of stress concentration. The ductility of the AZ91 strip was improved. However, the yield strength of the 221 Hz-EPT sample decreased slightly due to the reduction of the amount of β particles.

The XRD and SEM observation revealed that EPT tremendously accelerated the β→α phase transformation. Compared with the microstructure of the AT sample, it is obvious that the acceleration of the β→α phase transformation during EPT was not a result of the effect of rapid heating of electropulsing, but from the EPT itself. Previous studies[12–14] indicated that EPT enhanced nucleation of phase transformation by decreasing the thermodynamic barrier. This effect of electropusling on the phase transformation can be described with Eq. (1).[12]

$$\Delta G = \Delta G_0 + \Delta G_e$$
$$\Delta G_e = \mu_0 g \xi(\sigma_1, \sigma_2) j^2 \Delta V \quad , \qquad (1)$$

where ΔG is the free energy change for the β→α phase transformation, ΔG_0 is the change of free energy in a current-free system, ΔG_e is an energy change due to the change of distribution of the current in the formation of a nucleus, μ_0 is the magnetic susceptibility in vacuum, g is a positive geometric factor for coarse-grained materials, j is the current density, ΔV is the volume of a nucleus, and $\xi(\sigma_1, \sigma_2)$ is a factor that depends on the electrical properties of nucleus and medium, $\xi(\sigma_1, \sigma_2) = (\sigma_2 - \sigma_1)/(\sigma_1 + 2\sigma_2)$, where σ_1 and σ_2 are the conductivity of the α and β phase, respectively. During the β→α phase transformation, $(\sigma_\alpha = \sigma_1) > (\sigma_\beta = \sigma_2)$ results in $\xi(\sigma_1, \sigma_2) < 0$, therefore, $\Delta G_e < 0$ according to Eq. (1). This implies that EPT can accelerate the β→α phase transformation by decreasing the thermodynamic barrier.

During the spheroidization, the kinetics of the β→α phase transformation should be taken into account. For the AT samples, numerous β lamellar clusters still existed after conventional heat treatment. However, it took only about 7 s to complete the spheroidizing process in the aged AZ91 strip under 221 Hz-EPT, which had a similar heating rate to the AT sample by conventional heat treatment. The spheroidization of β particles depends critically on the diffusion of Al atom in the as-aged AZ91 strip under EPT. Previous studies[15] indicated that EPT tremendously accelerated Al atomic diffusion due to the coupling of the thermal effect and the athermal effect of EPT. During multiple continuous electropulses through the AZ91 strips, the average atomic flux per second can be described by Eq. (2).[15]

$$J = J_t + J_a = \frac{2\pi D_1}{\Omega \ln\left(\frac{R'}{r_0}\right)} \cdot \left(1 + \frac{\delta c}{c_0}\right) + \frac{2N \cdot D_1 \cdot Z^* \cdot e \cdot \rho \cdot f \cdot j_m \cdot \tau_p}{\pi k T}$$
$$J_t = \frac{2\pi D_l}{\Omega \ln\left(\frac{R'}{r_0}\right)} \cdot \left(1 + \frac{\delta c}{c_0}\right) J_a = \frac{2N \cdot D_l \cdot Z^* \cdot e \cdot \rho \cdot f \cdot j_m \cdot \tau_p}{\pi k T} \quad , \qquad (2)$$

where J_t is the flux of atoms resulting from the thermal activation effect during EPT and J_a is the flux of atoms contributed by the athermal effect of EPT, D_l is the lattice diffusion coefficient, c_0 is the average concentration of vacancy, δc is the supersaturation concentration of vacancies, Ω is the atom volume, r_0 and R' are the distance far from dislocation where the vacancy concentrations are c_0 and $c_0 + \delta c$, respectively; N is the atom density, Z^* is an effective valence, e is the electron charge, ρ is the resistivity, k is the Boltzmann constant, T is the absolute temperature; and j_m, f, and τ_p are peak current density, frequency, and duration of electropulsing, respectively.

According to Eq. (2), EPT increases the average atomic flux substantially due to the athermal effect of electropulsing, which is an additional high energy input through momentum transferred from electrons compared with conventional heat treatment. Furthermore, Eq. (2) reveals that j_a increases linearly with the three electric parameters, j_m, f, and τ_p. During EPT, the temperature of the sample increases with these three parameters because increases in j_m, f, and τ_p contribute to the larger Joule heating effect. Thus, increasing f, τ_p, j_m not only enhances the athermal effect, but also increases the thermal effect. A previous study[13] revealed that temperature was an important factor for the atomic flux, which accelerated the diffusional β→α phase transformation in the case of EPT since D_l increases exponentially with temperature T according to Eq. (3)[16]:

$$D_l = D_0 \exp\left(\frac{-Q}{RT}\right) \quad , \qquad (3)$$

where D_0 is the diffusion preexponential factor and Q is the activation energy. This implies that EPT tremendously accelerates the dissolution and spheroidization of the β phase in the as-aged AZ91 strip due to increase in the Al atom diffusion flux.

V. CONCLUSIONS

The electropulsing treatment (EPT) tremendously accelerated the spheroidization of the β phase in the aged AZ91 alloy strip during a very short time of 7 s. EPT increased the elongation to failure by about 80% without loss of tensile strength. A mechanism for rapid spheroidization of the β phase during EPT was proposed. EPT enhances the nucleation of the β→α phase transformation by decreasing the thermodynamic barrier. In addition, EPT increases the diffusion flux of Al atoms substantially as a result of the coupling of the thermal and athermal effects of EPT.

ACKNOWLEDGMENTS

The authors would like to thank the support from the Tsinghua-CityU Collaboration Scheme. The work was supported by the National Natural Science Foundation of China (No. 50571048) and Research Grant Council, Hong Kong SAR, China (Grant No. CityU 119908).

REFERENCES

1. P.B. Prangnell, J.R. Bowen, and P.J. Apps: Ultra-fine grain structures in aluminium alloys by severe deformation processing. *Mater. Sci. Eng., A* **178,** 375 (2004).
2. R.Z. Valiev, R.K. Islamgaliev, and I.V. Alexandrov: Bulk nanostructured materials from severe plastic deformation. *Prog. Mater. Sci.* **45,** 103 (2000).
3. C. Xu, M. Furukawa, Z. Horita, and T.G. Langdon: Severe plastic deformation as a processing tool for developing superplastic metals. *J. Alloys Compd.* **378,** 27 (2004).
4. V.N. Chuvil'deev, T.G. Nieh, M.Y. Gryazov, A.N. Sysoev, and V.I. Kopylov: Low-temperature superplasticity and internal friction in microcrystalline Mg alloys processed by ECAP. *Scr. Mater.* **50,** 861 (2004).
5. B. Chen, D.L. Lin, L. Jin, X.Q. Zeng, and C. Lu: Equal-channel angular pressing of magnesium alloy AZ91 and its effects on microstructure and mechanical properties. *Mater. Sci. Eng., A* **483–484,** 113 (2008).
6. M.T. Pérez-Prado, J.A. del Valle, and O.A. Ruano: Achieving high strength in commercial Mg cast alloys through large strain rolling. *Mater. Lett.* **59,** 3299 (2005).
7. M.T. Pérez-Prado, J.A. Del Valle, and O.A. Ruano: Grain refinement of Mg–Al–Zn alloys via accumulative roll bonding. *Scr. Mater.* **51,** 1093 (2004).
8. M.T. Pérez-Prado, J.A. Del Valle, J.M. Contreras, and O.A. Ruano: Microstructural evolution during large strain hot rolling of an AM60 Mg alloy. *Scr. Mater.* **50,** 661 (2004).
9. H. Conrad, N. Karam, and S. Mannan: Effect of electric-current pulses on the recrystallization of copper. *Scr. Metall.* **17,** 411 (1983).
10. H. Conrad: Effect of electric current on solid-state phase transformations in metals. *Mater. Sci. Eng., A* **287,** 227 (2000).
11. Z.H. Xu, G.Y. Tang, S.Q. Tian, F. Ding, and H.Y. Tian: Research of electroplastic rolling of AZ31 Mg alloy strip. *J. Mater. Process. Technol.* **182,** 128 (2007).
12. Y.Z. Zhou, W. Zhang, M.L. Sui, D.X. Li, G.H. He, and J.D. Guo: Formation of a nanostructure in a low-carbon steel under high current density electropulsing. *J. Mater. Res.* **17,** 921 (2002).
13. Y.Z. Zhou, J.D. Guo, W. Zhang, and G.H. He: Influence of electropulsing on nucleation during phase transformation. *J. Mater. Res.* **17,** 3012 (2002).
14. Y.Z. Zhou, W. Zhang, B.Q. Wang, and J.D. Guo: Ultrafine-grained microstructure in a Cu–Zn alloy produced by electropulsing treatment. *J. Mater. Res.* **18,** 1991 (2003).
15. Y.B. Jiang, G.Y. Tang, L. Guan, S.N. Wang, Z.H. Xu, C.H. Shek, and Y.H. Zhu: The effect of electropulsing treatment on the solid solution behavior of aged Mg alloy AZ61 strip. *J. Mater. Res.* **23,** 2685 (2008).
16. D.A. Porter and K.E. Easterling: *Phase Transformations in Metals and Alloys*, 2nd ed. (Chapman Hall, London, 1992), p. 68.